

Inhibition of p21-activated kinase rescues symptoms of fragile X syndrome in mice

Mansuo L. Hayashi*[†], B. S. Shankaranarayana Rao[‡], Jin-Soo Seo[§], Han-Saem Choi[§], Bridget M. Dolan*, Se-Young Choi[§], Sumantra Chattarji[¶], and Susumu Tonegawa*^{||}

*The Picower Institute for Learning and Memory, Howard Hughes Medical Institute, RIKEN–Massachusetts Institute of Technology Neuroscience Research Center, and Departments of Biology and Brain and Cognitive Sciences, Massachusetts Institute of Technology, Cambridge, MA 02139; [‡]Department of Neurophysiology, National Institute of Mental Health and Neurosciences, Bangalore 560029, India; [§]Department of Physiology, College of Dentistry, Seoul National University, Seoul 110-749 Korea; and [¶]National Center for Biological Sciences, Tata Institute of Fundamental Research, Bangalore 560065, India

Contributed by Susumu Tonegawa, May 29, 2007 (sent for review May 21, 2007)

Fragile X syndrome (FXS), the most commonly inherited form of mental retardation and autism, is caused by transcriptional silencing of the fragile X mental retardation 1 (FMR1) gene and consequent loss of the fragile X mental retardation protein. Despite growing evidence suggesting a role of specific receptors and biochemical pathways in FXS pathogenesis, an effective therapeutic method has not been developed. Here, we report that abnormalities in FMR1 knockout (KO) mice, an animal model of FXS, are ameliorated, at least partially, at both cellular and behavioral levels, by an inhibition of the catalytic activity of p21-activated kinase (PAK), a kinase known to play a critical role in actin polymerization and dendritic spine morphogenesis. Greater spine density and elongated spines in the cortex, morphological synaptic abnormalities commonly observed in FXS, are at least partially restored by postnatal expression of a dominant negative (dn) PAK transgene in the forebrain. Likewise, the deficit in cortical long-term potentiation observed in FMR1 KO mice is fully restored by the dnPAK transgene. Several behavioral abnormalities associated with FMR1 KO mice, including those in locomotor activity, stereotypy, anxiety, and trace fear conditioning are also ameliorated, partially or fully, by the dnPAK transgene. Finally, we demonstrate a direct interaction between PAK and fragile X mental retardation protein *in vitro*. Overall, our results demonstrate the genetic rescue of phenotypes in a FXS mouse model and suggest that the PAK signaling pathway, including the catalytic activity of PAK, is a novel intervention site for development of an FXS and autism therapy.

cortical long-term potentiation | spine morphology | trace fear conditioning | autism

Fragile X syndrome (FXS), the most commonly inherited form of mental retardation and the most common cause of autism, is caused by the loss of the fragile X mental retardation protein (FMRP) encoded by the *fragile X mental retardation 1 (FMR1)* gene (1). Although moderate to severe mental retardation and a developmental delay are the key features of FXS, patients also display problems related to anxiety, attention deficit, hyperactivity, stereotypy, seizure, and social behavior. *FMR1* knockout (KO) mice (2), which exhibit phenotypes similar to those seen in FXS in humans, have served as a useful model system for investigating how the absence of FMRP leads to the various molecular, cellular, and behavioral abnormalities observed in the disorder. Although these studies have led to valuable insights into the etiology of FXS, there has not been effective treatment of this debilitating disorder.

Several key observations are strongly suggestive of a primary role of defects in dendritic spines and synaptic plasticity in the symptoms associated with FXS (3). Increased numbers of dendritic spines and an abundance of long and immature spines have been reported in FXS individuals and *FMR1* KO mice (4–7). FMRP and its mRNA are found in dendrites and spines, the sites of transmission and plasticity at glutamatergic synapses in the brain (8). In addition, FMRP regulates mRNA translation, a key regulatory step in the maintenance of long-term synaptic plasticity (9, 10). Indeed, plas-

ticity at glutamatergic synapses, such as long-term potentiation (LTP) in the cortex and long-term depression in the hippocampus, is abnormal in *FMR1* KO mice (11–13).

The molecular underpinnings of spine abnormalities in FXS are not well understood. However, it is known that FMRP is a selective RNA-binding protein and can repress translation of the bound mRNA (9, 10, 14). Some of these mRNAs encode proteins that regulate spine morphology and/or synaptic function. In *Drosophila*, dFMR (the fly homologue of FMRP) binds to the mRNA encoding small GTPase dRac, a critical regulator of actin cytoskeletal remodeling (15). One of the main downstream effectors of Rac is p21-activated kinase (PAK), a family of serine–threonine kinases that is composed of at least three members, PAK1, PAK2, and PAK3 (16). Notably, loss-of-function mutations in the *PAK3* gene are associated with non-syndromic X-linked mental retardation (17, 18).

Strikingly, in transgenic (TG) mice in which PAK activity is inhibited by its dominant negative (dn) form (dnPAK), cortical spine morphology exhibits features that are opposite to those seen in FXS patients and *FMR1* KO mice (19). Specifically, cortical neurons in the dnPAK TG mice have fewer dendritic spines and a lower proportion of longer and thinner spines. These TG mice also exhibit enhanced cortical LTP in contrast to the reduced cortical LTP observed in *FMR1* KO mice. These findings give rise to the intriguing possibility that PAK and *FMR1* may antagonize each other to regulate spine morphology and synaptic function, and therefore an inhibition of PAK activity may lead to a correction of some of the symptoms associated with FXS. To test this hypothesis, we attempted to rescue a range of cellular and behavioral abnormalities observed in *FMR1* KO mice by using a genetic strategy to inhibit PAK activity.

Results

Experimental Strategy. Our strategy involved the generation of *FMR1* KO mice with inhibited PAK activity in the forebrain. To this end, we crossed dnPAK TG mice to *FMR1* KO mice to generate littermates with four different genotypes: WT, *FMR1* KO, dnPAK TG, and the double mutant dnPAK TG;*FMR1* KO

Author contributions: M.L.H., S.-Y.C., S.C., and S.T. designed research; M.L.H., B.S.S.R., J.-S.S., H.-S.C., and B.M.D. performed research; M.L.H., B.S.S.R., and S.-Y.C. analyzed data; and M.L.H., B.M.D., S.C., and S.T. wrote the paper.

The authors declare no conflict of interest.

Freely available online through the PNAS open access option.

Abbreviations: dn, dominant negative; *FMR1*, fragile X mental retardation 1; FMRP, fragile X mental retardation protein; FXS, fragile X syndrome; KO, knockout; LTP, long-term potentiation; PAK, p21-activated kinase; TG, transgenic; TBS, theta-burst stimulation.

[†]Present address: Department of Neuroscience Drug Discovery, Merck Research Laboratories, Boston, MA 02115.

^{||}To whom correspondence should be addressed. E-mail: tonegawa@mit.edu.

This article contains supporting information online at www.pnas.org/cgi/content/full/0705003104/DC1.

© 2007 by The National Academy of Sciences of the USA

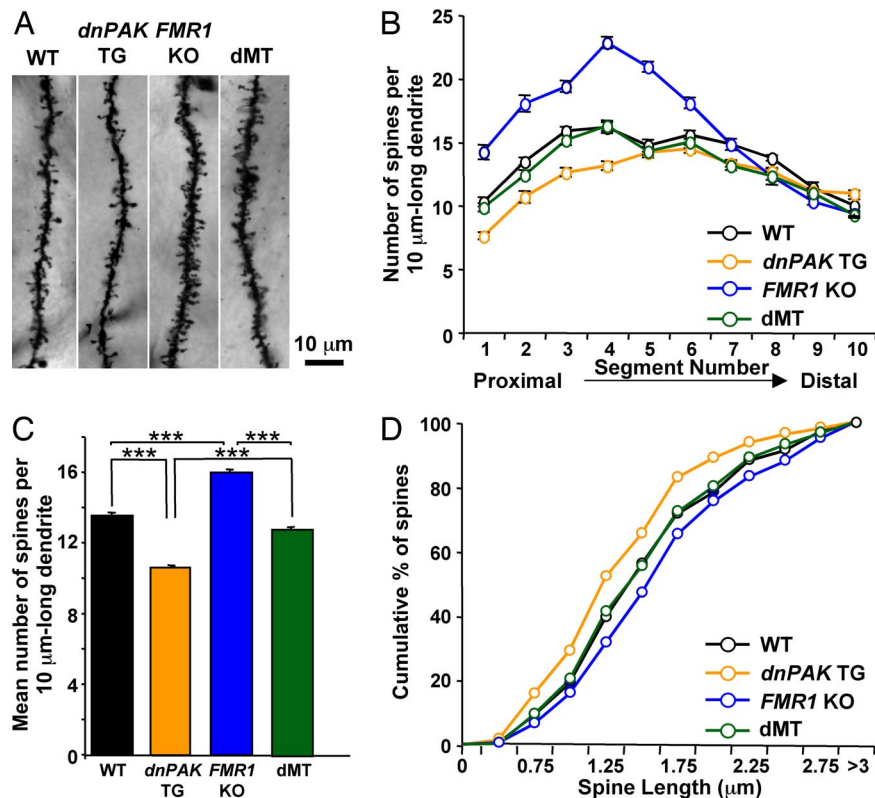


Fig. 1. PAK inhibition partially rescues increased density and length of dendritic spines in *FMR1* KO mice. (A) Representative dendritic segments of layer II/III pyramidal neurons from WT ($n = 20$ neurons; two mice), *dnPAK* TG mice ($n = 30$ neurons; three mice), *FMR1* KO mice ($n = 20$ neurons; two mice), and double mutant *dnPAK* TG;*FMR1* KO mice (dMT; $n = 40$ neurons; four mice). (B) On each primary apical dendritic branch, 10 consecutive 10 μm -long dendritic segments were analyzed to quantify spine density. Spine density in dMTs was comparable to WT controls in all dendritic segments except segments 7 and 8 ($P > 0.05$ in segments 1–6, 9, and 10; $P < 0.01$ in segments 7 and 8). (C) Mean spine density in dMTs (1.28 ± 0.02) was significantly lower than that in *FMR1* KO mice (1.60 ± 0.02 ; $P < 0.001$) and significantly higher than that in *dnPAK* TG mice (1.06 ± 0.01 ; $P < 0.001$). ANOVA, $P < 0.0001$. ***, $P < 0.001$. (D) As for spine length, *FMR1* KO neurons (444 spines) exhibited a significant shift in the overall spine distribution toward spines of longer length compared with WT neurons (406 spines; Kolmogorov-Smirnov test: $P < 0.05$), whereas *dnPAK* TG neurons (630 spines) exhibited the opposite shift to shorter spines ($P < 0.01$). In contrast, spine length distribution in dMT neurons (785 spines) overlapped well with WT neurons and is significantly different from *FMR1* KO neurons ($P < 0.01$).

mice (dMT mice). All four genotypes are maintained in C57/B6 background. In *dnPAK* TG mice, reduction in PAK activity does not start until the third postnatal week and reaches to $\approx 40\%$ inhibition at the second postnatal month, according to an assay of the level of active, autophosphorylated PAK (19). We assume the same developmental kinetics of PAK inhibition applies to dMT mice. As discussed earlier, our aim was to test the specific prediction that inhibiting PAK activity will rescue various phenotypes exhibited by the *FMR1* KO mice. All experiments and analyses were carried out “blind,” and the codes for the genotypes were broken only after analysis was completed.

PAK Inhibition Partially Rescues Increased Density and Length of Dendritic Spines in *FMR1* KO Mice. Because spine abnormality is a major pathological hallmark in FXS patients and *FMR1* KO mice at the cellular level, we first examined dendritic spine morphology by measuring spine density in apical dendrites of Golgi-stained layer II/III pyramidal neurons of the temporal cortex of dMT mice and their littermates, *dnPAK* TG, *FMR1* KO, and WT mice. We quantified the number of spines per 10 μm of dendritic segments that run proximal to distal to the neuronal soma. In proximal dendritic segments, spine density was lower in *dnPAK* TG mice compared with WT mice, whereas it was higher in *FMR1* KO mice compared with WT mice (Fig. 1A and B). In contrast, spine density in dMT mice was comparable to that in WT controls in all dendritic segments except segments 7 and 8 (Fig. 1B). When averaged over all segments, mean spine

density in dMT mice was significantly lower than that in *FMR1* KO mice and significantly higher than that in *dnPAK* TG mice (Fig. 1C). These results indicate that PAK inhibition partially restores the abnormality of spine density in *FMR1* KO mice.

In addition to an increased spine density, cortical neurons from FXS patients and *FMR1* KO mice exhibit increased spine length (4–7). To investigate whether *dnPAK* can also restore this abnormality, we measured spine length (the radial distance from tip of spine head to dendritic shaft) of Golgi-stained pyramidal neurons in the four genotypes. In cumulative frequency plots, *FMR1* KO neurons exhibited a significant shift in the overall spine distribution toward spines of longer length compared with WT neurons, whereas *dnPAK* TG neurons exhibited the opposite shift to shorter spines (Fig. 1D). In contrast, spine length distribution of dMT neurons overlapped well with that of WT neurons (Fig. 1D), indicating that PAK inhibition is sufficient to restore the cortical spine length abnormality in *FMR1* KO mice.

PAK Inhibition Rescues Reduced Cortical LTP in *FMR1* KO Mice. Cortical LTP has been shown to be reduced in *FMR1* KO mice, whereas it is enhanced in *dnPAK* TG mice (12, 13, 19). To assess the effect of PAK inhibition on the cortical synaptic transmission and plasticity in *FMR1* KO mice, we carried out extracellular field recordings in temporal cortex layer II/III synapses while stimulating layer IV. Basal synaptic transmission, as measured by field potential responses to a range of stimulus intensities, did not differ between the four genotypes (Fig. 2A). However, as

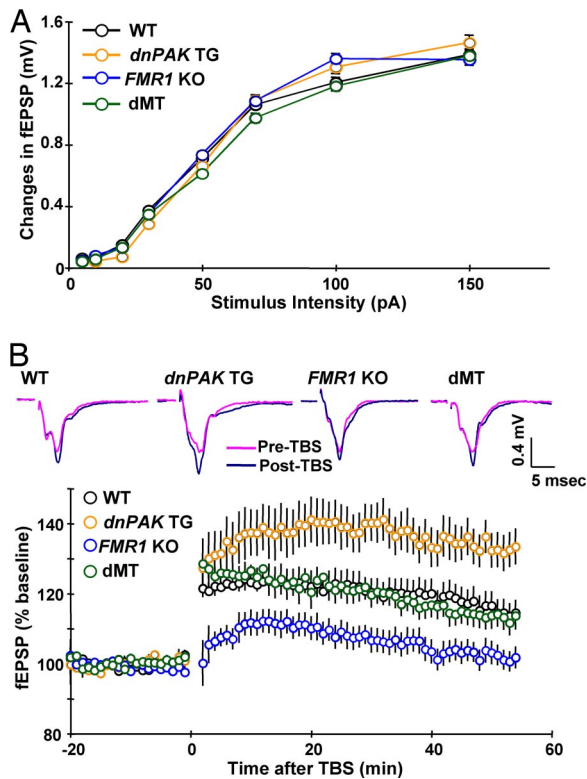


Fig. 2. PAK inhibition rescues reduced cortical LTP in *FMR1* KO mice. (A) Input–output curves plotting the changes in field excitatory postsynaptic potential (fEPSP) amplitude and their corresponding presynaptic stimulus intensity in WT ($n = 45$ slices; 16 mice), *dnPAK* TG ($n = 30$ slices; 10 mice), *FMR1* KO ($n = 57$ slices; 19 mice), and dMT mice ($n = 24$ slices; 8 mice). (B) Cortical LTP induced by TBS was enhanced in *dnPAK* TG ($n = 13$ slices; 11 mice), but reduced in *FMR1* KO ($n = 17$ slices; 11 mice), relative to WT controls ($n = 17$ slices; 11 mice); for responses at 55 min poststimulation, ANOVA, $P < 0.05$; for both *dnPAK* TG versus WT and *FMR1* KO versus WT, $P < 0.04$. By contrast, the magnitude of LTP was indistinguishable between dMT slices ($n = 13$ slices; 9 mice) and WT controls ($P > 0.05$ for responses at 55 min poststimulation). An overlay of representative field potential traces taken during baseline of recording and at 55 min poststimulation is shown for each genotype.

expected, administration of theta-burst stimulation (TBS) at 100 Hz produced LTP of a lower magnitude in *FMR1* KO mice than in WT mice and LTP of a higher magnitude in *dnPAK* TG than in WT mice (Fig. 2B). In contrast, the magnitude of LTP was indistinguishable between dMT mice and WT controls at various times after the application of the stimulus (Fig. 2B). This result demonstrated that PAK inhibition rescues LTP defects in *FMR1* KO mice.

PAK Inhibition Results in a Partial Rescue of Behavioral Abnormalities in *FMR1* KO Mice. Spine morphology and synaptic plasticity are thought to underlie learning and memory. To test whether the partial rescue of spine morphology and the complete rescue of cortical LTP by PAK inhibition could ameliorate behavioral deficits present in *FMR1* KO mice, the mice of various genotypes were subjected to a series of behavioral tasks. In an open-field test where mice are placed in a box and allowed to run freely for 10 min, *FMR1* KO mice exhibited three abnormal behaviors compared with WT mice (20): (i) hyperactivity; they traveled a longer distance and moved for a longer period (Fig. 3A and data not shown); (ii) stereotypy; they exhibited a higher number of repetitive behaviors (Fig. 3B); and (iii) hypoanxiety; they stayed in the center field for a longer period and in the corners of the field for a shorter period (Fig. 3C and data not shown). In all three behaviors, the dMT mice

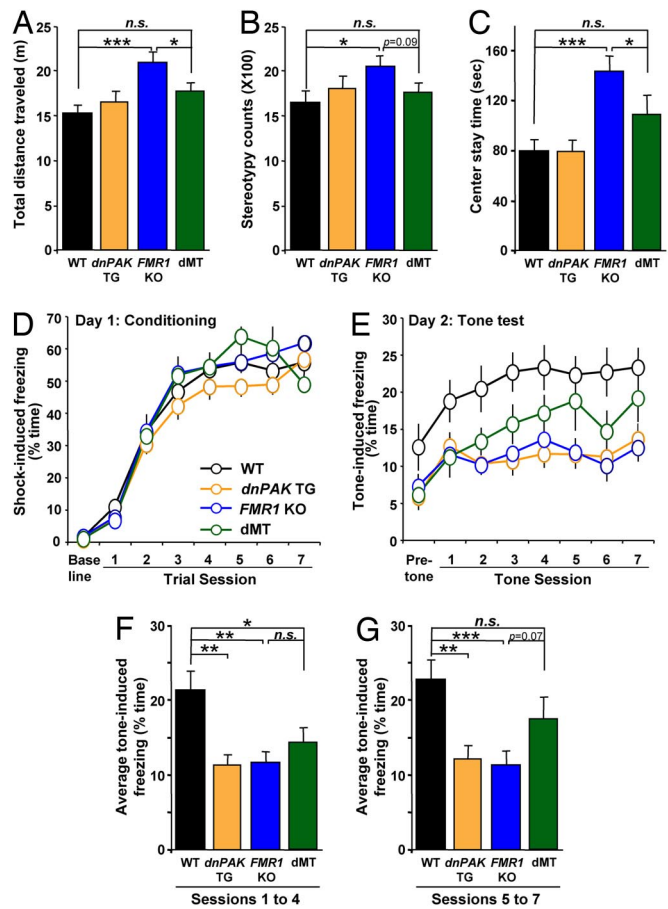


Fig. 3. PAK inhibition partially rescues behavioral abnormalities in *FMR1* KO mice. (A–C) Open-field test (WT, $n = 10$ mice; *dnPAK* TG, $n = 10$ mice; *FMR1* KO, $n = 11$ mice; dMT, $n = 11$ mice). n.s., not statistically different. *, $P < 0.05$; ***, $P < 0.001$. (A) *FMR1* KO traveled a longer distance compared with WT mice (ANOVA, $P < 0.01$; WT, 15.29 ± 0.92 m; *FMR1* KO, 20.99 ± 1.10 m, $P < 0.001$). (B) *FMR1* KO exhibited a higher number of repetitive behaviors than WT mice (stereotypy counts: ANOVA, $P < 0.05$; WT, $1,636 \pm 119$; *FMR1* KO, $2,049 \pm 125$, $P < 0.05$). (C) *FMR1* KO stayed a longer period in the center of the open field than WT mice (ANOVA, $P < 0.001$; WT, 79.8 ± 8.5 s; *FMR1* KO, 143.1 ± 12.0 s, $P < 0.001$). In all three behaviors, the dMT mice exhibited comparable performance to WT controls ($P > 0.05$ for all of the following parameters: distance traveled, 17.76 ± 0.91 m; stereotypy counts, $1,756 \pm 102$; and center time, 108.8 ± 14.6 s). (D–G) Trace fear conditioning task (WT, $n = 15$ mice; *dnPAK* TG, $n = 12$ mice; *FMR1* KO, $n = 15$ mice; dMT, $n = 9$ mice). n.s., not statistically different. *, $P < 0.05$; **, $P < 0.01$; ***, $P < 0.001$. (D) On day 1 (conditioning), the four genotypes of mice exhibited comparable amounts of freezing preconditioning (baseline) and postconditioning in all trials. (E) At the 24-h tone test, the four genotypes exhibited comparable amounts of pretone freezing (ANOVA $P > 0.05$). However, for tone-dependent freezing, *FMR1* KO mice and *dnPAK* TG mice exhibited a significant reduction compared with WT controls (ANOVA for each tone session, $P < 0.05$; for *FMR1* KO versus WT, $P < 0.05$ for session 1 and $P < 0.01$ for sessions 2–7; for *dnPAK* TG versus WT, $P > 0.05$ for session 1 and $P < 0.01$ for sessions 2–7). The dMT mice also showed freezing deficits during the first several tone sessions (sessions 1–4) compared with WT controls ($P < 0.05$). However, with additional tone sessions (sessions 5–7), freezing by dMT mice caught up to that of WT controls ($P > 0.05$). (F) Average freezing for sessions 1–4. ANOVA $P < 0.05$. The dMT mice showed freezing deficits compared with WT controls ($P < 0.05$), but the deficits in dMT mice were less pronounced compared with *dnPAK* TG ($P < 0.01$) or *FMR1* KO mice ($P < 0.01$). (G) Average freezing for sessions 5–7. ANOVA $P < 0.05$. Freezing level in dMT mice was not significantly different from WT controls ($P > 0.05$), and there were trends in its difference from *dnPAK* TG ($P = 0.12$) or *FMR1* KO mice ($P = 0.07$).

exhibited performance comparable to WT controls (Fig. 3A–C). This finding indicated that PAK inhibition in *FMR1* KO mice restores locomotion, repetitive behavior, and anxiety to WT levels.

To further examine whether PAK inhibition can rescue abnormal cortex-dependent behaviors, we conducted trace fear conditioning, a test that depends on the integrity of the prefrontal cortex and is sensitive to attention-distracting stimuli (21, 22). It was previously shown that *FMRI* KO mice are impaired in this form of conditioning, which may relate to the attention deficits in FXS patients (13). In this task, a conditioning trial was composed of a tone (as the conditioned stimulus), then a 30-s time gap (also called trace), and finally an electric shock (as the unconditioned stimulus). Seven trials were given to allow the mice to learn the association between the tone and the shock across the 30-s time gap. Mice that learn and remember this association will become immobile (or “freeze”) in response to the tone, even when they are placed into a new chamber with a different shape and smell compared with the training chamber. During training, the four genotypes exhibited comparable amounts of freezing in all conditioning trials (Fig. 3D), suggesting normal memory acquisition. However, when placed in a new chamber 24 h after training, both *FMRI* KO mice and *dnPAK* TG mice exhibited a significant reduction in tone-induced freezing compared with WT controls (Fig. 3E), indicating an impaired trace fear memory in these two genotypes. The dMT mice also showed freezing deficits during the first several tone sessions (sessions 1–4) compared with WT controls (Fig. 3E), although the deficits during these sessions were, on average, less pronounced compared with *dnPAK* TG or *FMRI* KO mice (Fig. 3F). However, with additional tone sessions (sessions 5–7), freezing by dMT caught up to that of WT, whereas its difference from *FMRI* KO mice almost reached statistical significance ($P = 0.07$; Fig. 3G). Thus, the dMT mice are slow in expressing the memory and/or require a repetition of the recall cue (tone), but they can eventually (after five tone sessions) recall the memory at the level that is not significantly different from the WT level.

PAK1 Interacts with FMRP. The morphological, electrophysiological, and behavioral data presented so far demonstrate that PAK inhibition is indeed capable of rescuing, at least partially, multiple abnormalities in *FMRI* KO mice. To begin to understand the underlying mechanism, we investigated whether PAK1 (the most abundant PAK in the brain) and FMRP physically interact. Because PAK1 and FMRP are both localized in synapses (8, 19), we prepared synapse-enriched membrane extract from the mouse brain and subjected the extract to immunoprecipitation with a PAK1 antibody (α -PAK1). Proteins that may coprecipitate through their direct or indirect interaction with PAK1 were separated by SDS/PAGE and subjected to Western blot analysis with an FMRP antibody. FMRP immunoreactivity was observed in PAK1 immunoprecipitates but not in control serum immunoprecipitates (Fig. 4A Upper). This interaction is specific because it did not occur when PAK1 antibody was preincubated with a blocking peptide, which competes with PAK1 for binding to the PAK1 antibody, before immunoprecipitation (Fig. 4A Upper). This result demonstrated that the endogenous PAK1 and FMRP interact, directly or indirectly, in the brain.

To examine whether PAK1 directly interacts with FMRP, we performed a GST pull-down assay in which *in vitro*-translated FMRP was incubated with either GST or GST-tagged PAK1 (GST-PAK1). GST-PAK1, but not GST alone, bound to FMRP [Fig. 4C and supporting information (SI) Fig. 5], suggesting a direct interaction between PAK1 and FMRP. FMRP contains a primary phosphorylation site at Ser-499 and three RNA-binding domains (KH1, KH2, and RGG) that are conserved among species (Fig. 4B) (1, 23). To map the PAK1-binding region on FMRP, we used a series of deletion or point mutants of FMRP in the GST pull-down assay. An FMRP mutant without the RGG box (Δ RGG) or phosphorylation domain containing Ser-499 (Δ S499) was still able to bind to PAK1, whereas an FMRP mutant without KH domains (Δ KH) or with a point mutation in

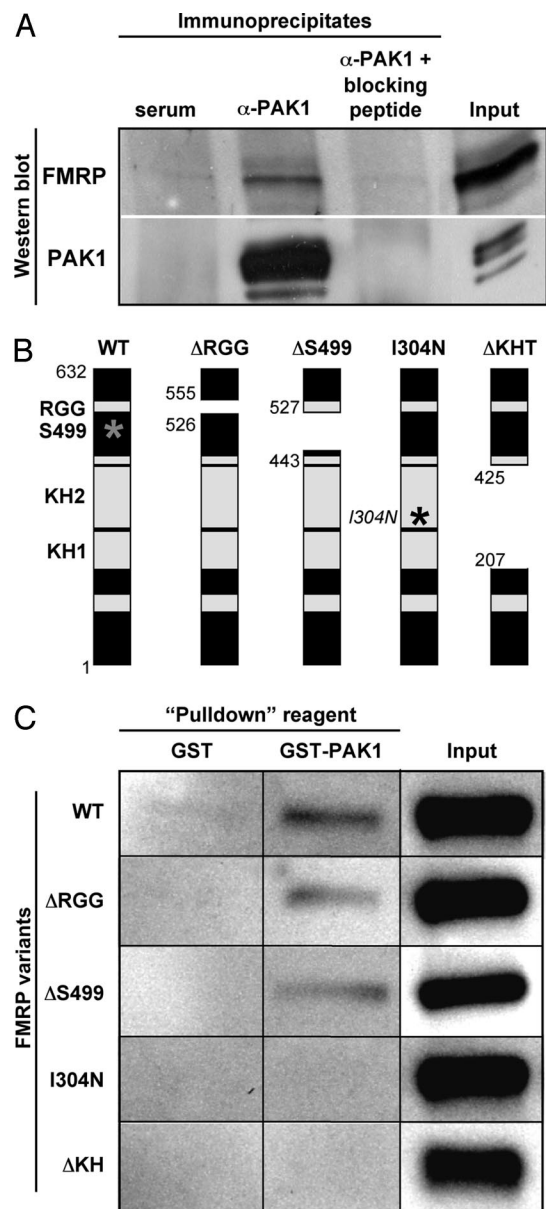


Fig. 4. PAK1 interacts with FMRP. (A) Immunoprecipitation followed by Western blot analysis. Brain extract was subjected to immunoprecipitation with either rabbit serum (negative control), PAK1 antibody (α -PAK1), or α -PAK1 plus a blocking peptide. Western blots were probed for either FMRP or PAK1. For Input, 2% of the extract used for a single immunoprecipitation was loaded on the gel. (B) Schematic structure of FMRP, highlighting various functional domains including three RNA-binding motifs (RGG, KH1, and KH2) and the phosphorylation site (S499, represented by a gray asterisk). The constructs used for *in vitro* binding included full-length (WT), truncated (Δ RGG, Δ S499, and Δ KH), or mutated (I304N) FMRP. Δ RGG refers to the FMRP variant with a deletion of the RGG box at amino acids 526–555. The deleted area in Δ S499 spans amino acids 443–527 and includes the phosphorylation site, S499, as well as putative phosphorylation sites. The isoleucine to asparagine missense mutation in the KH2 domain mimics that previously reported in a human FXS patient (I304N, represented by a black asterisk). The Δ KH deletion mutant lacks both KH domains in tandem corresponding to amino acids 207–425. The numbers refer to the amino acid positions designated by the SwissProt Q06787 entry. Adapted from ref. 38. (C) Characterization of the interaction between PAK1 and various FMRP variants *in vitro*. *In vitro*-translated FMRP variants were incubated with GST or GST-PAK1 and glutathione Sepharose beads. The complexes isolated by this method were subjected to SDS/PAGE and Western blotted for FMRP. For Input, 10% of *in vitro*-translated FMRP sample before the binding reaction was carried out was loaded on the gel.

the KH2 domain previously found in a human with severe FXS (I304N) (24) was unable to bind to PAK1 (Fig. 4B and C). These results suggested that PAK1 directly binds to FMRP and this interaction requires the integrity of the KH domains of FMRP.

Discussion

In this study, we demonstrate that postnatal inhibition of catalytic activity of PAK in the forebrain of *FMR1* KO mice ameliorates, at least partially, some of the FXS-related abnormalities present at the levels of synaptic morphology, synaptic plasticity, and behavior. We have also provided evidence suggesting that PAK and FMRP can physically interact. Taken together, these results demonstrate the genetic rescue of phenotypes in a FXS mouse model and identify postnatal PAK inhibition as a potential therapeutic strategy for countering the various debilitating symptoms of FXS and autism.

At the moment, we do not know the precise nature of the binding of PAK with FMRP nor the interaction between the signaling pathways involving these proteins. Our observation that inhibition of PAK kinase activity can counteract the deficits in *FMR1* KO mice suggests several possibilities. For instance, PAK may repress FMRP's activity by phosphorylating FMRP or an upstream regulator of FMRP or a downstream effector of FMRP. As previously shown, *FMR1* KO mice exhibit enhanced basal ERK phosphorylation (and presumably activity) (25), whereas ERK is phosphorylated and activated by PAK at least in non-neuronal cells (26). ERK is involved in regulation of spine morphology, synaptic plasticity, and behaviors (27, 28); therefore, it is possible that PAK inhibition returns the levels of phospho-ERK in *FMR1* KO mice to WT levels, thereby reversing phenotypes in *FMR1* KO mice. Alternatively, consistent with FMRP's role in repressing protein synthesis (9, 10, 14), FMRP may antagonize PAK-mediated signaling by binding to and repressing the translation of mRNAs encoding Rac1, the upstream activator of PAK, and possibly other components of the PAK pathway, including cytoplasmic FMRP interacting protein (CYFIP) and PAK itself (15, 29). Considering our *in vitro* evidence of a direct interaction between PAK1 and FMRP, it is also possible that active PAK1 binds to the KH domains of FMRP and thereby negatively regulates FMRP's activity by competing with mRNAs for binding to these domains. Obviously, further study is necessary to elucidate these mechanisms.

Our *in vivo* data in mice suggest that treatment of FXS patients by PAK inhibition after the appearance of disease symptoms may be possible. *FMR1* KO mice exhibit abnormalities as early as the first postnatal week (30, 31). On the other hand, we know that in *dnPAK* TG mice reduction of PAK activity does not start until the third postnatal week and reaches to $\approx 40\%$ inhibition only at the second postnatal month (19). Therefore, assuming the same developmental kinetics of PAK inhibition applies to dMT mice, our data suggest that the phenotypes of *FMR1* KO mice could be restored, at least partially, by PAK inhibition that did not take place until a few weeks after the appearance of disease symptoms. In human FXS patients, symptoms like developmental delay appear as early as 9–12 months of age and typically diagnosis follows shortly after (32, 33). This finding implies that PAK inhibition could be an effective postdiagnostic therapy for FXS children. PAK inhibitors like CEP-1343 have been described (34). Our findings warrant testing of these inhibitors in FXS animal models with a hope of an eventual development of an FXS drug.

In conclusion, although future studies will be necessary to further characterize the precise molecular nature of the interaction between PAK and FMRP, our findings clearly demonstrate that PAK and FMRP can exert opposing actions that form the functional basis for reversing several key cellular and behavioral symptoms of FXS. In addition to their significant therapeutic implications, these results add further evidence in

support of a primary, and potentially causal, role for defects in spine morphogenesis in mental retardation.

Methods

Golgi Analysis. Following the Golgi-Cox technique (35), 120- μ m-thick serial sections were obtained from the brains of 2-month-old male littermates. Layer II/III pyramidal neurons in the temporal cortex were visualized under an upright BX61 microscope (Olympus, Melville, NY) with a motorized XY stage using NeuroLucida/ stereology software (MicroBrightfield, Williston, VT). On each primary apical dendritic branch, 10 consecutive 10 μ m-long dendritic segments were analyzed to quantify spine density. To ensure sampling consistency between Golgi analysis and electrophysiological experiments, analyses in the temporal cortex were all carried out in slices or sections corresponding to figures 62–67 of the Mouse Brain Atlas (36).

Electrophysiology. From 3-month-old male littermates, coronal brain slices containing temporal cortex were prepared and left to recover for at least 1 h before recording in oxygenated (95% O₂ and 5% CO₂) warm (30°C) artificial cerebrospinal fluid containing 124 mM NaCl, 5 mM KCl, 1.25 mM NaH₂PO₄, 1 mM MgCl₂, 2 mM CaCl₂, 26 mM NaHCO₃, and 10 mM dextrose. Field potentials in layer II/III evoked by layer IV stimulation were measured as described (19), and responses were quantified as the amplitude of field potential in cortex. LTP was induced by TBS, which consisted of eight brief bursts (each with four pulses at 100 Hz) of stimuli delivered every 200 msec.

Open-Field Test. Two-month-old male littermates were subjected to the open-field test according to standard procedures. Each mouse ran for 10 min in a VersaMax activity monitor chamber (Accuscan Instruments, Columbus, OH). Open-field activity was detected by photobeam breaks and analyzed with VersaMax software. Stereotypy was recorded when the mouse broke the same beam (or set of beams) repeatedly. Stereotypy count is the number of beam breaks that occurred during this period of stereotypic activity.

Trace Fear Conditioning Task. Three-month-old male littermates were subjected to trace fear conditioning as described (13). On day 1, mice were placed in the training chamber (chamber A; Coulbourn Instruments, Allentown, PA) for 60 s before the onset of a 15-s white noise tone (conditioned stimulus). Thirty seconds later, mice received a 1-s shock (0.7-mA intensity; unconditioned stimulus). Thus, one trial is composed of tone (conditioned stimulus), 30 s of blank time (also called trace), and then shock (unconditioned stimulus). Seven trials with an inter-trial interval of 210 s were given to let the mice learn the association between tone and shock across a time gap. To examine whether mice remember this association, on day 2, mice were placed into a new chamber (chamber B) with a different shape and smell from those in chamber A. After 60 s, a 15-s tone was repeated seven times with an inter-trial interval of 210 s. Video images were digitized, and the percentage of freezing time during each inter-trial interval was analyzed with the Image FZ program (O'Hara & Co., Tokyo, Japan). Freezing was defined as the absence of all but respiratory movement for a 1-s period.

Immunoprecipitation and Western Blotting. Mouse brains were homogenized in ice-cold homogenization buffer [0.32 M sucrose/10 mM Tris-HCl, pH 7.4/5 mM EDTA/Complete Protease Inhibitor Mixture Tablets (Roche, Indianapolis, IN)] and centrifuged at 1,000 $\times g$ for 10 min at 4°C. The supernatant was collected and centrifuged at 21,000 $\times g$ for 15 min at 4°C. The pellet was resuspended in TE buffer (10 mM Tris-HCl pH 7.4/5 mM EDTA) and one-ninth volume of cold DOC buffer (500 mM Tris-HCl, pH 9.0/10% sodium deoxycholate) was added. The

mixture was incubated in a 37°C water bath for 30 min while shaking and mixed with one-ninth volume of buffer T (1% Triton X-100/1% sodium deoxycholate/500 mM Tris-HCl, pH 9.0). The membrane extract was dialyzed against binding/dialysis buffer (50 mM Tris-HCl, pH 7.4/0.1% Triton X-100) at 4°C overnight. For immunoprecipitation, the dialyzed membrane extract was precleared with protein A-Sepharose beads, then incubated with α -PAK1 (N-20; Santa Cruz Biotechnology, Santa Cruz, CA) or control rabbit serum (Sigma, St. Louis, MO) in binding/dialysis buffer for 3 h, and then incubated with protein A-Sepharose beads overnight at 4°C. To test binding specificity, α -PAK1 was also incubated with its corresponding blocking peptide (Santa Cruz Biotechnology) before incubation with the membrane extract. Proteins that bound to the beads were separated by SDS/PAGE and subjected to Western blot analysis with α -PAK1 antibody diluted at 1:1,000. For FMRP Western blots, the membrane was processed with the Blast blotting amplification system (PerkinElmer, Wellesley, MA) with α -FMRP antibody (Chemicon, Temecula, CA) diluted at 1:1,000.

GST Pull-Downs. GST-PAK1 plasmid was obtained from Joe Kissil (Wistar Institute, Philadelphia, PA) (37). Plasmids encoding FMRP and its mutants were obtained from Edouard Khandjian (Laval University, Quebec, Canada) (38). GST and GST-PAK1 proteins were expressed in BL21 *Escherichia coli*, purified on glutathione Sepharose 4B (GS4B) beads (Amersham Pharmacia, Piscataway, NJ), and dialyzed with PBS overnight. FMRP and its mutants were *in vitro*-translated with the TNT-coupled reticulocyte lysate systems kit (Promega, Madison, WI) and labeled with Transcend tRNA (Promega). GST or GST-PAK1

was incubated with FMRP or its mutants in binding buffer (50 mM Tris-HCl, pH 7.5/120 mM NaCl/10 mM MgCl₂/5% glycerol/1% Triton X-100) for 3 h. GS4B beads were added and incubated for 1 h. Proteins that bound to the beads were separated by SDS/PAGE and subjected to Western blot analysis with streptavidin-horseradish peroxidase to detect *in vitro*-translated FMRP or its mutants.

Animal Handling, Experimental Design, and Data Analysis. All strains of mice were of the C57/B6 background. *FMR1* KO mice were obtained from Steven Warren (Emory University, Atlanta, GA). *dnPAK* TG mice were generated in S.T.'s laboratory (19). Mouse maintenance and all experimental procedures were performed in compliance with National Institutes of Health guidelines. All experiments were conducted in a blind fashion. Unless specified otherwise, data were analyzed with Statview software (SAS, Cary, NC) using a one-way ANOVA test followed by Fisher's protected least significance difference posthoc test. Values are presented as mean \pm SEM.

We thank Wenjiang Yu and Frank Bushard for excellent technical assistance; Dr. Arvind Govindarajan for helpful discussions on the manuscript; Drs. Mark Bear (Massachusetts Institute of Technology), Steven Warren, Edouard Khandjian, and Joe Kissil for reagents; Joseph Titus for help in collating Golgi images; and Anupratap Tomar for help with analysis of spine data. S.C. is supported by the FRAXA Foundation and the Wellcome Trust. M.L.H. was supported by a postdoctoral fellowship from the FRAXA Foundation and the Simons Foundation. This work is supported by National Institutes of Health Grant RO1-MH78821 and National Institute of Mental Health Center Grant PH50-MH58880 (to S.T.).

- O'Donnell WT, Warren ST (2002) *Annu Rev Neurosci* 25:315–338.
- Dutch-Belgian Fragile X Consortium (1994) *Cell* 78:23–33.
- Grossman AW, Aldridge GM, Weiler IJ, Greenough WT (2006) *J Neurosci* 26:7151–7155.
- Hinton VJ, Brown WT, Wisniewski K, Rudelli RD (1991) *Am J Med Genet* 41:289–294.
- Comery TA, Harris JB, Willems PJ, Oostra BA, Irwin SA, Weiler IJ, Greenough WT (1997) *Proc Natl Acad Sci USA* 94:5401–5404.
- Irwin SA, Patel B, Idupulapati M, Harris JB, Crisostomo RA, Larsen BP, Kooy F, Willems PJ, Cras P, Kozlowski PB, et al. (2001) *Am J Med Genet* 98:161–167.
- McKinney BC, Grossman AW, Elisseeu NM, Greenough WT (2005) *Am J Med Genet B Neuropsychiatr Genet* 136:98–102.
- Weiler IJ, Irwin SA, Klintsova AY, Spencer CM, Brazelton AD, Miyashiro K, Comery TA, Patel B, Eberwine J, Greenough WT (1997) *Proc Natl Acad Sci USA* 94:5395–5400.
- Laggerbauer B, Ostareck D, Keidel EM, Ostareck-Lederer A, Fischer U (2001) *Hum Mol Genet* 10:329–338.
- Li Z, Zhang Y, Ku L, Wilkinson KD, Warren ST, Feng Y (2001) *Nucleic Acids Res* 29:2276–2283.
- Huber KM, Gallagher SM, Warren ST, Bear MF (2002) *Proc Natl Acad Sci USA* 99:7746–7750.
- Li J, Pelletier MR, Perez Velazquez JL, Carlen PL (2002) *Mol Cell Neurosci* 19:138–151.
- Zhao MG, Toyoda H, Ko SW, Ding HK, Wu LJ, Zhuo M (2005) *J Neurosci* 25:7385–7392.
- Mazroui R, Huot ME, Tremblay S, Filion C, Labelle Y, Khandjian EW (2002) *Hum Mol Genet* 11:3007–3017.
- Lee A, Li W, Xu K, Bogert BA, Su K, Gao FB (2003) *Development (Cambridge, UK)* 130:5543–5552.
- Bokoch GM (2003) *Annu Rev Biochem* 72:743–781.
- Allen KM, Gleeson JG, Bagrodia S, Partington MW, MacMillan JC, Cerione RA, Mulley JC, Walsh CA (1998) *Nat Genet* 20:25–30.
- Bienvenu T, des Portes V, McDonnell N, Carrie A, Zemni R, Couvert P, Ropers HH, Moraine C, van Bokhoven H, Fryns JP, et al. (2000) *Am J Med Genet* 93:294–298.
- Hayashi ML, Choi SY, Rao BS, Jung HY, Lee HK, Zhang D, Chattarji S, Kirkwood A, Tonegawa S (2004) *Neuron* 42:773–787.
- Peier AM, McIlwain KL, Kenneson A, Warren ST, Paylor R, Nelson DL (2000) *Hum Mol Genet* 9:1145–1159.
- McEchron MD, Bouwmeester H, Tseng W, Weiss C, Disterhoft JF (1998) *Hippocampus* 8:638–646.
- Han CJ, O'Tuathaigh CM, van Trigt L, Quinn JJ, Fanselow MS, Mongeau R, Koch C, Anderson DJ (2003) *Proc Natl Acad Sci USA* 100:13087–13092.
- Ceman S, O'Donnell WT, Reed M, Patton S, Pohl J, Warren ST (2003) *Hum Mol Genet* 12:3295–3305.
- Feng Y, Absher D, Eberhart DE, Brown V, Malter HE, Warren ST (1997) *Mol Cell* 1:109–118.
- Hou L, Antion MD, Hu D, Spencer CM, Paylor R, Klann E (2006) *Neuron* 51:441–454.
- Eblen ST, Slack JK, Weber MJ, Catling AD (2002) *Mol Cell Biol* 22:6023–6033.
- Selcher JC, Nekrasova T, Paylor R, Landreth GE, Sweatt JD (2001) *Learn Mem* 8:11–19.
- Kelleher RJ, III, Govindarajan A, Jung HY, Kang H, Tonegawa S (2004) *Cell* 116:467–479.
- Schenck A, Bardoni B, Langmann C, Harden N, Mandel JL, Giangrande A (2003) *Neuron* 38:887–898.
- Nimchinsky EA, Oberlander AM, Svoboda K (2001) *J Neurosci* 21:5139–5146.
- Galvez R, Greenough WT (2005) *Am J Med Genet A* 135:155–160.
- Bailey DB, Jr, Skinner D, Sparkman KL (2003) *Pediatrics* 111:407–416.
- Baranek GT, Danks CD, Skinner ML, Bailey DB, Jr, Hatton DD, Roberts JE, Mirrett PL (2005) *J Autism Dev Disord* 35:645–656.
- Nheu TV, He H, Hirokawa Y, Tamaki K, Florin L, Schmitz ML, Suzuki-Takahashi I, Jorissen RN, Burgess AW, Nishimura S, et al. (2002) *Cancer J* 8:328–336.
- Ramon-Moliner E (1970) *Contemporary Research Methods in Neuroanatomy* (Springer, Berlin).
- Franklin KBJ, Paxinos G (1997) *The Mouse Brain in Stereotaxic Coordinates* (Academic, San Diego).
- Kissil JL, Wilker EW, Johnson KC, Eckman MS, Yaffe MB, Jacks T (2003) *Mol Cell* 12:841–849.
- Mazroui R, Huot ME, Tremblay S, Boilard N, Labelle Y, Khandjian EW (2003) *Hum Mol Genet* 12:3087–3096.